Published in final edited form as:
Dev Biol. 2010 February 15; 338(2): 183. doi:10.1016/j.ydbio.2009.11.034.

Fgf8b-containing spliceforms, but not *Fgf8a*, are essential for *Fgf8* function during development of the midbrain and cerebellum

Qiuxia Guo, **Kairong Li**, **N. Abimbola Sunmonu**, and **James Y.H. Li***
Department of Genetics and Developmental Biology, University of Connecticut Health Center, 263 Farmington Avenue, Farmington, CT 06030

Summary

The single *Fgf8* gene in mice produces eight protein isoforms (Fgf8a–h) with different N-termini by alternative splicing. Gain-of-function studies have demonstrated that Fgf8a and Fgf8b have distinct activities in the developing midbrain and hindbrain (MHB) due to their different binding affinities with FGF receptors. Here we have performed loss-of-function analyses to determine the in vivo requirement for these two *Fgf8* spliceforms during MHB development. We showed that deletion of *Fgf8b*-containing spliceforms (*b*, *d*, *f* and *h*) leads to loss of multiple key regulatory genes, including *Fgf8* itself, in the MHB region. Therefore, specific inactivation of *Fgf8b*-containing spliceforms, similar to the loss of *Fgf8*, in MHB progenitors results in deletion of the midbrain, isthmus, and cerebellum. We also created a splice-site mutation abolishing *Fgf8a*-containing spliceforms (*a*, *c*, *e*, and *g*). Mice lacking *Fgf8a*-containing spliceforms exhibit growth retardation and postnatal lethality, and the phenotype is variable in different genetic backgrounds, suggesting that the *Fgf8a*-containing spliceforms may play a role in modulating the activity of *Fgf8*. Surprisingly, no discernable defect was detected in the midbrain and cerebellum of *Fgf8a*-deficient mice. To determine if *Fgf17*, which is expressed in the MHB region and possesses similar activities to *Fgf8a* based on gain-of-function studies, may compensate for the loss of *Fgf8a*, we generated *Fgf17* and *Fgf8a* double mutant mice. Mice lacking both *Fgf8a*-containing spliceforms and *Fgf17* display the same defect in the posterior midbrain and anterior cerebellum as *Fgf17* mutant mice. Therefore, *Fgf8b*-containing spliceforms, but not *Fgf8a*, are essential for the function of *Fgf8* during the development of the midbrain and cerebellum.

Keywords

Fgf8; alternative splicing; midbrain; cerebellum; organizer; signaling

Introduction

Alternative splicing occurs in 40–60% of the genes in humans and mice (Modrek and Lee, 2002). It is believed that alternative splicing significantly increases the complexity of the RNA and protein products expressed by the mammalian genome and allows an additional layer of control of gene function. However, the biological significance of alternative splicing of most mammalian genes is largely unexamined. Studies of the in vivo function of alternative splicing

*Author for correspondence: Department of Genetics and Developmental Biology, University of Connecticut Health Center, 263 Farmington Avenue, Farmington, CT 06030, jali@uchc.edu, Phone: (860) 679-3836, Fax: (860) 679-8345.

of key developmental regulators should provide important insight into the regulation and function of these molecules during development.

Fibroblast growth factor 8 (Fgf8), which belongs to the fibroblast growth factor (FGF) family, plays a key role in regulating different developmental processes (Itoh and Ornitz, 2008). Deletion of *Fgf8* in mice leads to catastrophic consequences during gastrulation, in addition to latter roles in the development of the central nervous system, sensory system, heart, limbs, jaws and teeth (Chi et al., 2003; Frank et al., 2002; Garel et al., 2003; Lewandoski et al., 2000; Moon and Capecchi, 2000; Storm et al., 2003; Sun et al., 2002; Sun et al., 1999; Trumpp et al., 1999). One of the best-studied functions of *Fgf8* is in formation of the midbrain and cerebellum, which develop from two adjacent segments of the neural tube called the mesencephalon (mes) and rhombomere 1 (r1), respectively (Wurst and Bally-Cuif, 2001). The dorsal mes gives rise to the superior colliculus and inferior colliculus, which process visual and auditory information, respectively, whereas dorsal r1 forms the cerebellum, which coordinates motor activity. Embryological and genetic studies have demonstrated that the expression of *Fgf8* in the mes/r1 junction, known as the isthmic organizer, patterns the mes and r1 and coordinates the growth and differentiation of the midbrain and cerebellum (Sato et al., 2004; Wurst and Bally-Cuif, 2001). Deletion of *Fgf8* in the mes/r1 region results in cell death between E8.5 and E9.5, and eventual loss of the entire midbrain, isthmus, and cerebellum by E18.5 (Chi et al., 2003).

The vertebrate *Fgf8* gene undergoes alternative splicing to produce eight possible spliceforms (a–h) that encode protein isoforms with different N-termini (Crossley and Martin, 1995; MacArthur et al., 1995; Sato et al., 2001). Previous studies have shown that two of the evolutionarily conserved Fgf8 isoforms, Fgf8a and Fgf8b, possess distinct activities (Sato et al., 2004). In mouse and chick embryos, misexpression of *Fgf8a* results in overgrowth of the mes and transforms the posterior forebrain into a midbrain fate (Lee et al., 1997; Liu et al., 1999; Sato et al., 2001). By contrast, misexpression of *Fgf8b* transforms the mes into a cerebellar fate (Liu et al., 1999; Sato et al., 2001). The remarkably different activities of these two Fgf8 isoforms can be exclusively attributed to a single amino acid in Fgf8b, which forms an additional binding site and thus increases affinity for FGFRs (Olsen et al., 2006). Analyses of mouse embryos lacking *Fgf8b*-containing spliceforms (*b, d, f,* and *h*) have demonstrated that these *Fgf8* spliceforms are essential for the function of *Fgf8* before gastrulation, but that the remaining *Fgf8a*-containing spliceforms (*a, c, e* and *g*) can partially compensate for the loss of *Fgf8b*-containig spliceforms in promoting mesoderm migration through the primitive streak in a dosage-dependent manner (Guo and Li, 2007). Experiments in Xenopus embryos have shown that *Fgf8a* plays an important role in the formation of the posterior neural tissue and induction of neural crest (Fletcher et al., 2006; Hong et al., 2008). The above observations suggest that *Fgf8a* and *Fgf8b* may work in concert to determine the function of *Fgf8* in vertebrate development. However, it remains unknown whether *Fgf8a* and *Fgf8b* have different contributions to *Fgf8* function during organogenesis in mice.

Fgf17, which is closely related to *Fgf8*, is expressed in a broad domain around the isthmus between E8.5 and E15.5 (Xu et al., 2000). Gain-of-function studies have demonstrated that Fgf17 has similar activity to Fgf8a (Liu et al., 2003; Olsen et al., 2006). Deletion of *Fgf17* leads to partial loss of the posterior midbrain and anterior cerebellum in mice, and removal of one copy of *Fgf8* enhances the tissue loss in the anterior cerebellum of *Fgf17* null mutant mice (Xu et al., 2000). These observations suggest that there may be synergistic interactions between *Fgf8a* and *Fgf17* in coordinating growth and differentiation of the cerebellum.

To determine the in vivo requirement for *Fgf8a* and *Fgf8b* during development of the midbrain and cerebellum, we have examined formation of these brain structures in mice lacking *Fgf8b*-containing spliceforms in tissue-specific conditional mutant mice. We also created a mutation

abolishing *Fgf8a*-containing spliceforms in mice to determine the requirement for *Fgf8a*. Finally, by generating double mutant mice that lack *Fgf17* and *Fgf8a-containing spliceforms*, we investigated the genetic interactions between *Fgf17* and *Fgf8a* during development of the midbrain and cerebellum. Our studies demonstrate the distinct requirement for the two sets of *Fgf8* spliceforms, containing *Fgf8a* or *Fgf8b*, in the overall function of *Fgf8*.

Materials and Methods

Generation of a mouse line deficient for Fgf8a

Using gene targeting, we introduced a point mutation into the 3′ alternative splice acceptor of *Fgf8* exon 1D, changing the sequence from cagCATGTG to caaCATGTG (Fig. 3A). The mutation produces a new restriction endonuclease site for *Pci*I without altering the final amino acid sequence. A selectable marker, *neo* was placed 400 bp downstream of exon 1D. Targeted embryonic stem cells carrying the mutation, designated as $Fgf8^{\Delta a\text{-}neo}$, were identified by Southern blot, PCR and restriction analysis, and used to generate germline chimeras. The *neo* cassette, which was flanked by two *loxP* sites, was subsequently removed using a germ-line *CMV-Cre* mouse line (Li et al., 2002), producing a new allele called $Fgf8^{\Delta a}$ (Fig. 3A).

Mouse breeding and genotyping

Noon of the day on which the vaginal plug was found was designated as embryonic day 0.5 (E0.5). Embryos between E8.5 and E9.5 were staged according to the number of somites. All mouse lines were maintained on an outbred CD1 genetic background unless stated otherwise (Charles River Lab, Wilmington, MA). To produce C57BL/6J congenic animals, $Fgf8^{+/\Delta a}$ or $Fgf8^{+/\Delta b}$ mice were backcrossed with C57BL/6J mice (the Jackson Laboratory, Bar Harbor, ME) for at least seven generations. Genotypes of mice were determined by PCR.

RNA in situ hybridization and histochemistry

For tissue preparation, embryonic brains were fixed by immersion in 4% paraformaldehyde (PFA) at 4°C for 3–16 hours. Postnatal mice were deeply anesthetized and transcardially perfused with 4% PFA. Brains were postfixed in the same fixative overnight at 4°C. For frozen tissue sections, brains were cryoprotected in 30% sucrose in PBS before rapid freezing in OCT compound (TissueTek) and sectioned with freezing microtome. Standard protocols for X-gal staining, in situ hybridization, and immunofluorescence on sections or in whole mount embryos were used (Nagy, 2003). Detailed protocols are available on the Li lab website (http://www.genetics.uchc.edu/lilab/Pages/Protocols.html). Analysis of cell death was performed by Nile Blue Sulfate staining of wholemount embryos as described previously (Chi et al., 2003). Antibodies used in the study are as follows: rabbit anti-TH (Pel-Freez, Rogers, AR), goat anti-5-HT (ImmunoStar, Hudson, WI), and Alexa fluorescent secondary antibodies (Invitrogen, Carlsbad, CA).

Results

Fgf8b spliceform is essential for Fgf8 function during MHB development

We have previously shown that $Fgf8^{\Delta b/\Delta b}$ embryos, which lack *Fgf8b*, *d*, *f* and *h* spliceforms (defined as *Fgf8b*-containing spliceforms), display severe abnormalities and growth retardation at E9.5 (Guo and Li, 2007). To circumvent the early embryonic lethality of $Fgf8^{\Delta b/\Delta b}$ embryos, we combined the $Fgf8^{\Delta b}$ allele with a conditional *Fgf8* mutant allele, $Fgf8^{F}$ (Meyers et al., 1998), and an $En1^{Cre}$ knock-in allele (Kimmel et al., 2000). In embryos carrying the $En1^{Cre}$ allele, the expression of Cre leads to recombination in cells throughout the mes/r1 area between the 3- to 10-somite stage (Li et al., 2002), so that the remaining wild-type *Fgf8* allele is deleted

and thus only *Fgf8a*-containing spliceforms (*a, c, e, and g*) are expressed in the mes/r1 of $Fgf8^{\Delta b/F}$; $En1^{+/Cre}$ embryos, designated as *Fgf8b* conditional knockout (*Fgf8b*-CKO).

$Fgf8^{\Delta b/F}$ mice were normal, but $Fgf8^{\Delta b/F}$; $En1^{+/Cre}$ mice died at birth. Examination of $Fgf8^{\Delta b/F}$; $En1^{+/Cre}$ embryos at E18.5 revealed a nearly complete loss of the midbrain and the cerebellum (Fig. 1B). The phenotype is remarkably similar to that found in $Fgf8^{-/F}$; $En1^{+/Cre}$ embryos with conditional deletion of *Fgf8* (Fig. 1C)(Chi et al., 2003). To compare the extent of MHB tissue loss between *Fgf8b*-CKO and *Fgf8*-CKO mice, we introduced a Cre-reporter allele, $R26R^{+}$ (Soriano, 1999), into these conditional mutant mice so that mes/r1 cells would be permanently marked by β-gal activity. Analysis of β-gal activity by X-gal histochemistry revealed that the entire mes/r1 area was populated by labeled cells in control embryos of genotype $Fgf8^{+/F}$; $En1^{+/Cre}$; $R26R^{+/-}$ at E10.5 and E18.5 (Fig. 1D and G). In both *Fgf8b*-CKO and *Fgf8*-CKO embryos, the mid-hindbrain domain demarcated by β-gal activity was reduced to a narrow stripe (Fig. 1E, F, H, and I). The residual X-gal positive domain was comparable between *Fgf8b*-CKO and *Fgf8*-CKO embryos at E18.5 (Fig. 1H–I). To analyze development of the mes/r1 basal plate, we examined the formation of dopaminergic and serotonergic neurons around the MHB junction (Zervas et al., 2004) by immunofluorescence with antibodies against tyrosine hydroxylase (TH) and *5*-hydroxytryptamine (5-HT). As described previously (Chi et al., 2003), dopaminergic neurons were largely depleted in the substantia nigra and ventral tegmental area (SN-VTA) of *Fgf8*-CKO embryos at E18.5 (Fig. 1L). Furthermore, there was a noticeable reduction in the number of serotonergic neurons in the raphe nuclei (Fig. 1J and L). Similar to *Fgf8*-CKO embryos, *Fgf8b*-CKO embryos at E18.5 exhibited an almost complete loss of dopaminergic neurons in the SN-VTA area, and a reduction of serotonergic neurons in raphe nuclei (Fig. 1K). Together, our data show that the *Fgf8b*-containing spliceforms are essential for *Fgf8* activity in MHB development.

Fgf8b-containing spliceforms are essential for maintaining the genetic cascade in the mes/r1 area

It has been shown that the expression of *Wnt1, Gbx2, Fgf17, En1,* and *Spry2* is lost in the mes/r1 region of $Fgf8^{-/F}$; $En1^{+/Cre}$ embryos between the 11- and 15-somite stages (Chi et al., 2003). To determine if *Fgf8b*-containing spliceforms are essential for *Fgf8* signaling to maintain the expression of these mes/r1 genes, we performed RNA in situ hybridization on $Fgf8^{\Delta b/F}$; $En1^{Cre/+}$ and control littermates between the 11- and 14-somite stages. Transcripts of *Fgf8* were detected in the isthmus of $Fgf8^{\Delta b/F}$; $En1^{Cre/+}$; $R26R^{+/-}$ embryos at the 11-somite stage, but were missing by the 14-somite stages (Fig. 2B and data not shown). At the 14-somite stage, *Wnt1* and *Gbx2* are normally expressed in two apposing transverse stripes in the posterior mes and anterior r1, respectively (Fig. 2C and E). In addition, *Wnt1* is expressed in dorsal midline, except for in r1 region, of the neural tube (Fig. 2C). The transverse stripes of *Wnt1* and *Gbx2* expression at the mes/r1 border were lost in $Fgf8^{\Delta b/F}$; $En1^{Cre/+}$ embryos at the 14-somite stage (Fig. 2D and F). However, *Wnt1* expression in the dorsal midline of the neural plate persisted and was abnormally expanded through presumptive r1 (Fig. 2D). The expression of *En1* and *Fgf17* was absent or greatly diminished at the mes/r1 region of $Fgf8^{\Delta b/F}$; $En1^{Cre/+}$ embryos at the 13–14 somite stages (Fig. 2H and J). These changes in gene expression in *Fgf8b*-CKO embryos are remarkably similar to those reported in *Fgf8*-CKO mutants (Chi et al., 2003). We examined two additional markers for mes/r1. The homeobox gene *Dmbx1* is expressed in the mes and diencephalon (Fig. 2K) (Ohtoshi et al., 2002). *Spry2*, which is a downstream target and feedback inhibitor of Fgf8 signaling, is expressed in the posterior mes and the metencephalon (Fig. 2M)(Liu et al., 2003). No expression of *Dmbx1* and *Spry2* was detected in mes/r1, whereas their expression in the diencephalon and the posterior metencephalon, respectively, was maintained in $Fgf8^{\Delta b/F}$; $En1^{Cre/+}$ embryos at the 13-somite stages (Fig. 2L and N). As described in *Fgf8*-CKO embryos (Chi et al., 2003), Nile Blue sulfate staining, which specifically marks dying cells, revealed a significant increase in the number of

dead cells in the mes and to a less extent in r1 of *Fgf8*$^{+/F}$; *En1*$^{Cre/+}$ embryos at the 13-somite stage (Fig. 2P). These data show that inactivation of *Fgf8b* in mes/r1 results in very similar responses in both gene expression and cell death to those found in the *Fgf8*-CKO embryos. Our results thus demonstrate that *Fgf8b*-containing spliceforms are essential for *Fgf8* function in maintaining the mes/r1 genetic cascade and the survival of mes/r1 cells.

Deletion of Fgf8a-containing spliceforms results in growth retardation and postnatal lethality in mice

Because deletion of *Fgf8b* leads to loss of the expression of *Fgf8a* and all other remaining *Fgf8* spliceforms in the isthmus by E9.5, we were unable to determine whether *Fgf8a* plays any role in the development of the midbrain and cerebellum. To address this question, we abolished *Fgf8a* expression by introducing a point mutation (designated as *Fgf8*$^{\Delta a}$) at the 3′ alternative splice acceptor of *Fgf8* exon 1D in mice (Fig. 3A). RT-PCR demonstrated that the transcripts of *Fgf8a*-containing spliceforms (*a*, *c*, *e*, and *g*) were missing, while *Fgf8b*-contaiing spliceforms, which utilize the remaining alternative splice acceptor of the exon 1D, are expressed in *Fgf8*$^{\Delta a/\Delta a}$ embryos at E8.5 (Fig. 3B).

Most *Fgf8*$^{\Delta a/\Delta a}$ mice on a CD1 outbred background were viable. However, adult *Fgf8*$^{\Delta a/\Delta a}$ mice (6-week or older) were smaller in size (Fig. 3C), and the average body weight of *Fgf8*$^{\Delta a/\Delta a}$ mutants was significantly lower than that of wild type or heterozygous littermates at E18.5 and postnatal day 24 (P24) (Fig. 3D). Some *Fgf8*$^{\Delta a/\Delta a}$ mice (14 out of 86 pups) were found dead before weaning, and the number of *Fgf8*$^{\Delta a/\Delta a}$ mice recovered at weaning was significantly lower than expected according to Mendelian inheritance (Table Ia). However, embryos of different genotypes from intercrosses between *Fgf8*$^{+/\Delta a}$ mice were recovered at normal ratios (Table Ib), suggesting that the homozygous mutation of *Fgf8*$^{\Delta a}$ results in partial lethality after birth. Interestingly, compared with wild-type controls, *Fgf8*$^{+/\Delta a}$ mice tended to have a lower body weight (Fig. 3C). On a C57BL/6J genetic background, few *Fgf8*$^{\Delta a/\Delta a}$ mice were recovered, and the number of *Fgf8*$^{+/\Delta a}$ mice was significantly reduced ($p<0.039$, X^2 test) (Table Ic). We examined matings between wild-type and *Fgf8*$^{+/\Delta a}$ or *Fgf8*$^{+/\Delta b}$ mice, and recovered normal numbers of *Fgf8*$^{+/\Delta b}$ pups, but *Fgf8*$^{+/\Delta a}$ pups were significantly fewer than that predicted by Mendelian ratios ($p<0.029$, X^2 test) (Table Id–e). Since both *Fgf8*$^{\Delta a}$ and *Fgf8*$^{\Delta b}$ alleles contain the same residual *loxP* site and are genotyped by the same method (see Materials and Methods), the observed reduction of *Fgf8*$^{+/\Delta a}$ mice is unlikely due to an adverse effect of the *loxP* sequence left in the intron of *Fgf8*$^{\Delta a}$ allele, or errors of PCR genotyping. Collectively, our results demonstrate that the deletion of *Fgf8a*-containing spliceforms leads to growth retardation and postnatal lethality, and the phenotype of *Fgf8*$^{+/\Delta a}$ and *Fgf8*$^{\Delta a/\Delta a}$ mice is more severe on a C57BL/6J versus CD1 background.

Fgf8a-containing spliceforms are dispensable for the development of the midbrain and cerebellum

To determine if *Fgf8a* is essential for the development of the mes/r1, we examined the midbrain and cerebellum of *Fgf8*$^{\Delta a/\Delta a}$ mutants at E18.5 and P15. The histology of the superior colliculus, inferior colliculus, and the cerebellum, which are derived from the alar plate of mes/r1, was indistinguishable among *Fgf8*$^{\Delta a/\Delta a}$, *Fgf8*$^{+/\Delta a}$, and their wild-type littermates (Fig. 4A–D). Immunofluorescence analysis of TH and 5-HT showed no obvious alterations of dopaminergic neurons and serotonergic neurons in the ventral midbrain and pons of *Fgf8*$^{\Delta a/\Delta a}$ embryos at E15.5 (Fig. 4E–F). Furthermore, we performed whole-mount immunohistochemistry using an anti-neurofilament antibody to examine the cranial nerves and their associated ganglia that derived from the MHB region. The formation of the cranial nerves (III–XI), their associated ganglia, and peripheral nerves was indistinguishable between *Fgf8*$^{\Delta a/\Delta a}$ and wild-type embryos at E10.5 and E11.5 (Fig. 4K–L and data not shown). These data collectively suggest that both the alar and basal plates of mes/r1 develop normally without *Fgf8a*-containing spliceforms.

We next generated *En1*$^{Cre/+}$*; Fgf8*$^{\Delta a/F}$*; R26R*$^{+/-}$ mice to specifically remove *Fgf8a*-containing spliceforms in the mes/r1 region. These mutant mice were normal in size, demonstrating that the growth retardation of *Fgf8*$^{\Delta a/\Delta a}$ mutants is caused by a defect outside the MHB region. No difference in the size of the midbrain and the cerebellum, which were marked by X-gal histochemistry, was observed between *En1*$^{Cre/+}$*; Fgf8*$^{\Delta a/F}$*; R26R*$^{+/-\Delta}$and *En1*$^{Cre/+}$*; Fgf8*$^{\Delta a/+}$*; R26R*$^{+/-}$ littermates at E16.5 or P15 (Fig. 4G–J).

To examine the patterning and growth of the mes/r1, we analyzed expression of MHB markers in *Fgf8*$^{\Delta a/\Delta a}$ embryos at E8.5, E9.5, and E10.5. Normal expression of *Gbx2, En1, Wnt1,* and *Fgf8* (*Fgf8b, d, f* and *h* only) was found in the mes/r1 region between E8.5 and E10.5, suggesting that loss of *Fgf8a*-containing spliceforms does not affect patterning of the mes/r1 (Fig. 5B and data not shown). *Spry1* and *Spry2* are expressed in two gradients diminishing from the isthmus in the mes/r region (Fig. 5C, and data not shown), and the expression of these two genes is considered a readout of Fgf8 signaling (Liu et al., 2003). No noticeable difference in the expression of *Spry1* and *Spry2* was found in the mes/r1 region of *Fgf8*$^{\Delta a/\Delta a}$ embryos at E9.5 and E10.5 (Fig. 5D and data not shown). To determine the size of the mes, we analyzed the expression of two homeobox genes, *Meis2* and *Dmbx1,* which are expressed in the mes and other areas of the neural tube (Fig. 5E and G) (Cecconi et al., 1997;Gogoi et al., 2002;Oulad-Abdelghani et al., 1997). The expression domains of *Meis2* and *Dmbx1* in the mes were indistinguishable between control and *Fgf8*$^{\Delta a/\Delta a}$ embryos at E10.5 (Fig. 5F and H). Our data collectively demonstrate that deletion of *Fgf8a*-containing spliceforms does not result in noticeable change in patterning and growth of the mes/r1, and that *Fgf8a*-containing spliceforms are dispensable for the formation of the midbrain and cerebellum.

Fgf17 dose not interacts with Fgf8a-containing spliceforms in the regulation of MHB development

Previous studies have demonstrated that there are genetic interactions between *Fgf8* and *Fgf17* (Xu et al., 2000). Furthermore, gain-of-function studies showed that *Fgf8a* and *Fgf17* have similar biological activity (Liu et al., 2003; Olsen et al., 2006). To determine if *Fgf17* may compensate for the loss of *Fgf8a* in *Fgf8*$^{\Delta a/\Delta a}$ mice, we examined the formation of the midbrain and the cerebellum in mutant mice with *Fgf8*$^{\Delta a}$ mutation on an *Fgf17*-null background.

Histology of the midbrain and cerebellum was examined around 5 weeks after birth, when these brain structures have fully matured. As described previously (Xu et al., 2000), the tissue between the inferior colliculus and the anterior cerebellum was significantly reduced in adult *Fgf17*$^{-/-}$ mice (Fig. 6B). Although there were variations in the size and the pattern of lobules I–III among wild-type mice, lobules I–III were truncated and considerably smaller in size in adult *Fgf17*$^{-/-}$ mice (Fig. 6B). Significantly, no additional reduction was detected in the inferior colliculus and the lobules I–III in the cerebellar vermis in *Fgf8*$^{+/\Delta a}$*; Fgf17*$^{-/-}$ (n=11) or *Fgf8*$^{\Delta a/\Delta a}$*; Fgf17*$^{-/-}$ mice (n=5) compared with *Fgf17*$^{-/-}$ mice (Fig. 6C and data not shown). These data demonstrate that *Fgf8a* and *Fgf17* do not play redundant roles in development of the midbrain and cerebellum.

Discussion

Previous studies using a gain-of-function approach have shown that the two *Fgf8* splice variants *Fgf8a* and *Fgf8b* have distinct inductive activities in mes/r1 fate specification (Lee et al., 1997; Liu et al., 1999; Sato et al., 2001). In chick embryos, expression of *Fgf8a* and *Fgf8b* are co-expressed in the isthmus (Sato and Nakamura, 2004). Furthermore, we observed that all eight *Fgf8* splice variants are co-expressed in the mes/r1 region of mouse embryos between E8.5 and E16.5 (Li and Li, manuscript in preparation). However, the in vivo function of these *Fgf8* spliceforms has not been examined. Using a loss-of-function approach, we have

determined the in vivo requirement for two complementary sets of *Fgf8* spliceforms containing *Fgf8a* or *Fgf8b* in development of the midbrain and cerebellum in mice, and uncovered molecular and cellular processes differentially regulated by each set of spliceforms.

We previously showed that deletion of *Fgf8b*-containing spliceforms results in a similar but significantly less severe phenotype than that of *Fgf8*-null mutant embryos during gastrulation (Guo and Li, 2007). Furthermore, in $Fgf8^{\Delta b/\Delta b}$ embryos at the early somite stage, region-specific markers, such as *Otx2*, *Gbx2*, *En1*, and *Fgf8*, are normally expressed in the neuroepithelium. These results demonstrate that *Fgf8a*-containing spliceforms are able to partially compensate for the loss of *Fgf8b*, and that *Fgf8b*-containing spliceforms are not essential for the induction of these mes/r1 genes (Guo and Li, 2007). In this study, we show that remaining *Fgf8* transcripts were lost in the mes/r1 region of $Fgf8^{\Delta b/F}; En1^{+/Cre}$ embryos between the 11- to 14-somite stages (Fig. 2B and data not shown). Thereafter, specific deletion of *Fgf8b*-containing spliceforms in the mes/r1 area results in a nearly complete deletion of the dorsal midbrain and the cerebellum, similar to the phenotype resulted from specific deletion of *Fgf8* in the isthmus. Since $Fgf8^{\Delta b/F}; En1^{+/Cre}$ embryos have only one functional *Fgf8a* copy, it is formally possible that two copies of *Fgf8a* is necessary to compensate for the loss of *Fgf8b*. However, we found that *Fgf8* expression were also lost in the isthmus in rare $Fgf8^{\Delta b/\Delta b}$ embryos that had survived to E9.5 (n=3/33), even though they had two copies of *Fgf8a* (supplementary figure S1). Therefore, our results from deletion of *Fgf8b*-containing spliceforms throughout the embryos or specifically in the mes/r1 area clearly demonstrate that *Fgf8b*-containing spliceforms are absolutely necessary to maintain the expression of *Fgf8* in the isthmus, and the remaining *Fgf8a*-containing spliceforms are not sufficient to compensate for the loss of *Fgf8b*-containing spliceforms.

Given the potent activity of *Fgf8a* in promoting the growth and differentiation of the midbrain (Lee et al., 1997; Liu et al., 1999; Sato et al., 2001), it is surprising that the midbrain develops normally in the absence of *Fgf8a*-containing spliceforms (Fig. 5). Our examination has not revealed any discernable abnormalities in the morphology, histology, and cellular specification and differentiation of the midbrain and the cerebellum of $Fgf8^{\Delta a/\Delta a}$ and $En1^{+/Cre}; Fgf8^{\Delta a/F}$ conditional mutant mice. In addition, we found that mice double homozygous for $Fgf8^{\Delta a}$ and *Fgf17*-null mutations display the same MHB phenotype as *Fgf17*-null mice (Fig. 6). These genetic data demonstrate that *Fgf17* does not compensate for the loss of *Fgf8a* in $Fgf8^{\Delta a/\Delta a}$ and *Fgf8a*-CKO mice, though overexpression of *Fgf8a* or *Fgf17* produces a similar phenotype in the mes/r1 area (Liu et al., 2003; Olsen et al., 2006; Xu et al., 2000). Our results demonstrate that *Fgf8a*-containing spliceforms are largely dispensable for the development of the midbrain and cerebellum.

How do *Fgf8b*-containing spliceforms achieve the overall activity of *Fgf8* in directing development of the midbrain and cerebellum? It has been proposed that the differentiation of the midbrain and cerebellum is controlled by distinct levels of FGF signaling. Although ectopic expression of *Fgf8b* transforms the mes into a cerebellar fate, low-level expression of *Fgf8b* results in a similar phenotype as ectopic expression of *Fgf8a* or *Fgf17* (Liu et al., 2003; Sato et al., 2001). Furthermore, a genetic study in which *Spry2*, an inhibitor of FGF signaling, was misexpressed in the mes/r1 region provide evidence that the regionalization of the embryonic midbrain and cerebellum is regulated by different levels of FGF signaling (Basson et al., 2008). Multiple inhibitors of FGF signaling, including Sprouty proteins (Minowada et al., 1999), Sef (Lin et al., 2002), Flrt1/3 (Haines et al., 2006), and Mpk3 (Klock and Herrmann, 2002), are expressed in the mes/r1 region in vertebrates. Significantly, *Spry1* and *Spry2* are induced by *Fgf8b* but not *Fgf8a* in mes/r1 cells in chick (Liu et al., 2003). Therefore, graded Fgf8b signaling shaped by feedback inhibition or graded Fgf8b protein concentration established by diffusion from the *Fgf8*-expressing cells in the isthmus may be sufficient to control the growth and patterning of the mes/r1 region. It is worth noting that multiple *Fgf8*

spliceforms, *Fgf8b, d, f and h*, are deleted in $Fgf8^{\Delta b/\Delta b}$ mutants, and these spliceforms are still expressed in $Fgf8^{\Delta a/\Delta a}$ mice. *Fgf8d, f and h*, whose activity has not been examined in mes/r1 cells, may interact with *Fgf8b* to constitute the overall function of *Fgf8* and contribute to compensate for the loss of *Fgf8a* in $Fgf8^{\Delta a/\Delta a}$ mice.

Deletion of *Fgf8a*-containing spliceforms, results in growth retardation and partial postnatal lethality (Fig. 3). Our preliminary results also indicate that these mutant mice have reduced fertility (data not shown). Interestingly, all these phenotypes are more severe on the C57BL/6J than the CD1 outbred background. The precise cause of the mutant phenotype and strain-dependent phenotypic variation remains to be determined. Nevertheless, our findings indicate that *Fgf8a*-containing spliceforms may have a functional role in *Fgf8*-expressing tissues outside the mes/r1. Abnormalities in the alternative splicing of *FGF8* affecting the production of *FGF8a* or *FGF8e* (there are no equivalents to *Fgf8c* and *Fgf8g* in humans) may contribute to growth retardation or neonatal lethality in humans.

Knockdown experiments using morpholino oligonucleotides have revealed that *Fgf8a* plays an important role in posterior neural specification in *X. laevis* and *X. tropicalis* embryos (Fletcher et al., 2006). However, no discernable abnormality in the central and peripheral nervous system was detected by marker analysis and neurofilament immunohistochemistry in $Fgf8^{\Delta a/\Delta a}$ embryos at E8.5 and E10.5 (Fig. 4K, L and data not shown). Therefore, loss of *Fgf8a* does not produce obvious defects in posterior neural specification in mice. The discrepancy in the mutant phenotype due to the loss of *Fgf8a* in mice and Xenopus might result from the different experimental approaches or a real difference between mouse and Xenopus Fgf8 isoform function.

Supplementary Material

Refer to Web version on PubMed Central for supplementary material.

Acknowledgments

We are grateful to Drs. Sohyun Ahn, Alexandra Joyner, and Mark Zervas for critical reading of the manuscript. We thank Dr. David Ornitz for providing the *Fgf17* mutant mice, Drs. Gail Martin and Alexandra Joyner for providing the $Fgf8^{F}$ and $En1^{Cre}$ mice, and the Gene Targeting and Transgenic Facility (GTTF) at UConn Health Center for the generation of $Fgf8^{\Delta a}$ mutant mice. We thank Drs. Richard Behringer and Alexandra Joyner for providing probes for RNA in situ hybridization. J. Li is supported by grants from the NIH and March of Dimes foundation.

References

Basson MA, Echevarria D, Ahn CP, Sudarov A, Joyner AL, Mason IJ, Martinez S, Martin GR. Specific regions within the embryonic midbrain and cerebellum require different levels of FGF signaling during development. Development 2008;135:889–98. [PubMed: 18216176]

Cecconi F, Proetzel G, Alvarez-Bolado G, Jay D, Gruss P. Expression of Meis2, a Knotted-related murine homeobox gene, indicates a role in the differentiation of the forebrain and the somitic mesoderm. Dev Dyn 1997;210:184–90. [PubMed: 9337138]

Chi CL, Martinez S, Wurst W, Martin GR. The isthmic organizer signal FGF8 is required for cell survival in the prospective midbrain and cerebellum. Development 2003;130:2633–2644. [PubMed: 12736208]

Crossley PH, Martin GR. The mouse Fgf8 gene encodes a family of polypeptides and is expressed in regions that direct outgrowth and patterning in the developing embryo. Development 1995;121:439–51. [PubMed: 7768185]

Crossley PH, Martinez S, Martin GR. Midbrain development induced by FGF8 in the chick embryo. Nature 1996;380:66–8. [PubMed: 8598907]

Fletcher RB, Baker JC, Harland RM. FGF8 spliceforms mediate early mesoderm and posterior neural tissue formation in Xenopus. Development 2006;133:1703–14. [PubMed: 16554360]

Frank DU, Fotheringham LK, Brewer JA, Muglia LJ, Tristani-Firouzi M, Capecchi MR, Moon AM. An Fgf8 mouse mutant phenocopies human 22q11 deletion syndrome. Development 2002;129:4591–603. [PubMed: 12223415]

Garel S, Huffman KJ, Rubenstein JL. Molecular regionalization of the neocortex is disrupted in Fgf8 hypomorphic mutants. Development 2003;130:1903–14. [PubMed: 12642494]

Gogoi RN, Schubert FR, Martinez-Barbera JP, Acampora D, Simeone A, Lumsden A. The paired-type homeobox gene Dmbx1 marks the midbrain and pretectum. Mech Dev 2002;114:213–7. [PubMed: 12175514]

Guo Q, Li JY. Distinct functions of the major Fgf8 spliceform, Fgf8b, before and during mouse gastrulation. Development 2007;134:2251–60. [PubMed: 17507393]

Haines BP, Wheldon LM, Summerbell D, Heath JK, Rigby PW. Regulated expression of FLRT genes implies a functional role in the regulation of FGF signalling during mouse development. Dev Biol 2006;297:14–25. [PubMed: 16872596]

Hong CS, Park BY, Saint-Jeannet JP. Fgf8a induces neural crest indirectly through the activation of Wnt8 in the paraxial mesoderm. Development 2008;135:3903–10. [PubMed: 18997112]

Inouye M, Oda SI. Strain-specific variations in the folial pattern of the mouse cerebellum. J Comp Neurol 1980;190:357–62. [PubMed: 7381062]

Itoh N, Ornitz DM. Functional evolutionary history of the mouse Fgf gene family. Dev Dyn 2008;237:18–27. [PubMed: 18058912]

Kimmel RA, Turnbull DH, Blanquet V, Wurst W, Loomis CA, Joyner AL. Two lineage boundaries coordinate vertebrate apical ectodermal ridge formation. Genes Dev 2000;14:1377–89. [PubMed: 10837030]

Klock A, Herrmann BG. Cloning and expression of the mouse dual-specificity mitogen-activated protein (MAP) kinase phosphatase Mkp3 during mouse embryogenesis. Mech Dev 2002;116:243–7. [PubMed: 12128234]

Lee SM, Danielian PS, Fritzsch B, McMahon AP. Evidence that FGF8 signalling from the midbrain-hindbrain junction regulates growth and polarity in the developing midbrain. Development 1997;124:959–69. [PubMed: 9056772]

Lewandoski M, Sun X, Martin GR. Fgf8 signalling from the AER is essential for normal limb development. Nat Genet 2000;26:460–3. [PubMed: 11101846]

Li JY, Lao Z, Joyner AL. Changing requirements for Gbx2 in development of the cerebellum and maintenance of the mid/hindbrain organizer. Neuron 2002;36:31–43. [PubMed: 12367504]

Lin W, Furthauer M, Thisse B, Thisse C, Jing N, Ang SL. Cloning of the mouse Sef gene and comparative analysis of its expression with Fgf8 and Spry2 during embryogenesis. Mech Dev 2002;113:163–8. [PubMed: 11960706]

Liu A, Li JY, Bromleigh C, Lao Z, Niswander LA, Joyner AL. FGF17b and FGF18 have different midbrain regulatory properties from FGF8b or activated FGF receptors. Development 2003;130:6175–85. [PubMed: 14602678]

Liu A, Losos K, Joyner AL. FGF8 can activate Gbx2 and transform regions of the rostral mouse brain into a hindbrain fate. Development 1999;126:4827–38. [PubMed: 10518499]

MacArthur CA, Lawshe A, Xu J, Santos-Ocampo S, Heikinheimo M, Chellaiah AT, Ornitz DM. FGF-8 isoforms activate receptor splice forms that are expressed in mesenchymal regions of mouse development. Development 1995;121:3603–13. [PubMed: 8582274]

Martinez S, Crossley PH, Cobos I, Rubenstein JL, Martin GR. FGF8 induces formation of an ectopic isthmic organizer and isthmocerebellar development via a repressive effect on Otx2 expression. Development 1999;126:1189–200. [PubMed: 10021338]

Meyers EN, Lewandoski M, Martin GR. An Fgf8 mutant allelic series generated by Cre- and Flp-mediated recombination. Nat Genet 1998;18:136–41. [PubMed: 9462741]

Minowada G, Jarvis LA, Chi CL, Neubuser A, Sun X, Hacohen N, Krasnow MA, Martin GR. Vertebrate Sprouty genes are induced by FGF signaling and can cause chondrodysplasia when overexpressed. Development 1999;126:4465–75. [PubMed: 10498682]

Modrek B, Lee C. A genomic view of alternative splicing. Nat Genet 2002;30:13–9. [PubMed: 11753382]

Moon AM, Capecchi MR. Fgf8 is required for outgrowth and patterning of the limbs. Nat Genet 2000;26:455–9. [PubMed: 11101845]

Nagy, A.; Gertsenstein, M.; Vintersten, K.; Behringer, R. Manipulating the Mouse Embryo. Cold Spring Harbor Laboratory Press; Cold Spring Harbor, New York: 2003.

Ohtoshi A, Nishijima I, Justice MJ, Behringer RR. Dmbx1, a novel evolutionarily conserved paired-like homeobox gene expressed in the brain of mouse embryos. Mech Dev 2002;110:241–4. [PubMed: 11744391]

Olsen SK, Li JY, Bromleigh C, Eliseenkova AV, Ibrahimi OA, Lao Z, Zhang F, Linhardt RJ, Joyner AL, Mohammadi M. Structural basis by which alternative splicing modulates the organizer activity of FGF8 in the brain. Genes Dev 2006;20:185–198. [PubMed: 16384934]

Oulad-Abdelghani M, Chazaud C, Bouillet P, Sapin V, Chambon P, Dolle P. Meis2, a novel mouse Pbx-related homeobox gene induced by retinoic acid during differentiation of P19 embryonal carcinoma cells. Dev Dyn 1997;210:173–83. [PubMed: 9337137]

Sato T, Araki I, Nakamura H. Inductive signal and tissue responsiveness defining the tectum and the cerebellum. Development 2001;128:2461–9. [PubMed: 11493563]

Sato T, Joyner AL, Nakamura H. How does Fgf signaling from the isthmic organizer induce midbrain and cerebellum development? Dev Growth Differ 2004;46:487–94. [PubMed: 15610138]

Sato T, Nakamura H. The Fgf8 signal causes cerebellar differentiation by activating the Ras-ERK signaling pathway. Development 2004;131:4275–85. [PubMed: 15294862]

Soriano P. Generalized lacZ expression with the ROSA26 Cre reporter strain [letter]. Nat Genet 1999;21:70–1. [PubMed: 9916792]

Storm EE, Rubenstein JL, Martin GR. Dosage of Fgf8 determines whether cell survival is positively or negatively regulated in the developing forebrain. Proc Natl Acad Sci U S A 2003;100:1757–62. [PubMed: 12574514]

Sun X, Mariani FV, Martin GR. Functions of FGF signalling from the apical ectodermal ridge in limb development. Nature 2002;418:501–8. [PubMed: 12152071]

Sun X, Meyers EN, Lewandoski M, Martin GR. Targeted disruption of Fgf8 causes failure of cell migration in the gastrulating mouse embryo. Genes Dev 1999;13:1834–46. [PubMed: 10421635]

Trumpp A, Depew MJ, Rubenstein JL, Bishop JM, Martin GR. Cre-mediated gene inactivation demonstrates that FGF8 is required for cell survival and patterning of the first branchial arch. Genes Dev 1999;13:3136–48. [PubMed: 10601039]

Wurst W, Bally-Cuif L. Neural plate patterning: upstream and downstream of the isthmic organizer. Nat Rev Neurosci 2001;2:99–108. [PubMed: 11253000]

Xu J, Liu Z, Ornitz DM. Temporal and spatial gradients of Fgf8 and Fgf17 regulate proliferation and differentiation of midline cerebellar structures. Development 2000;127:1833–43. [PubMed: 10751172]

Zervas M, Millet S, Ahn S, Joyner AL. Cell behaviors and genetic lineages of the mesencephalon and rhombomere 1. Neuron 2004;43:345–57. [PubMed: 15294143]

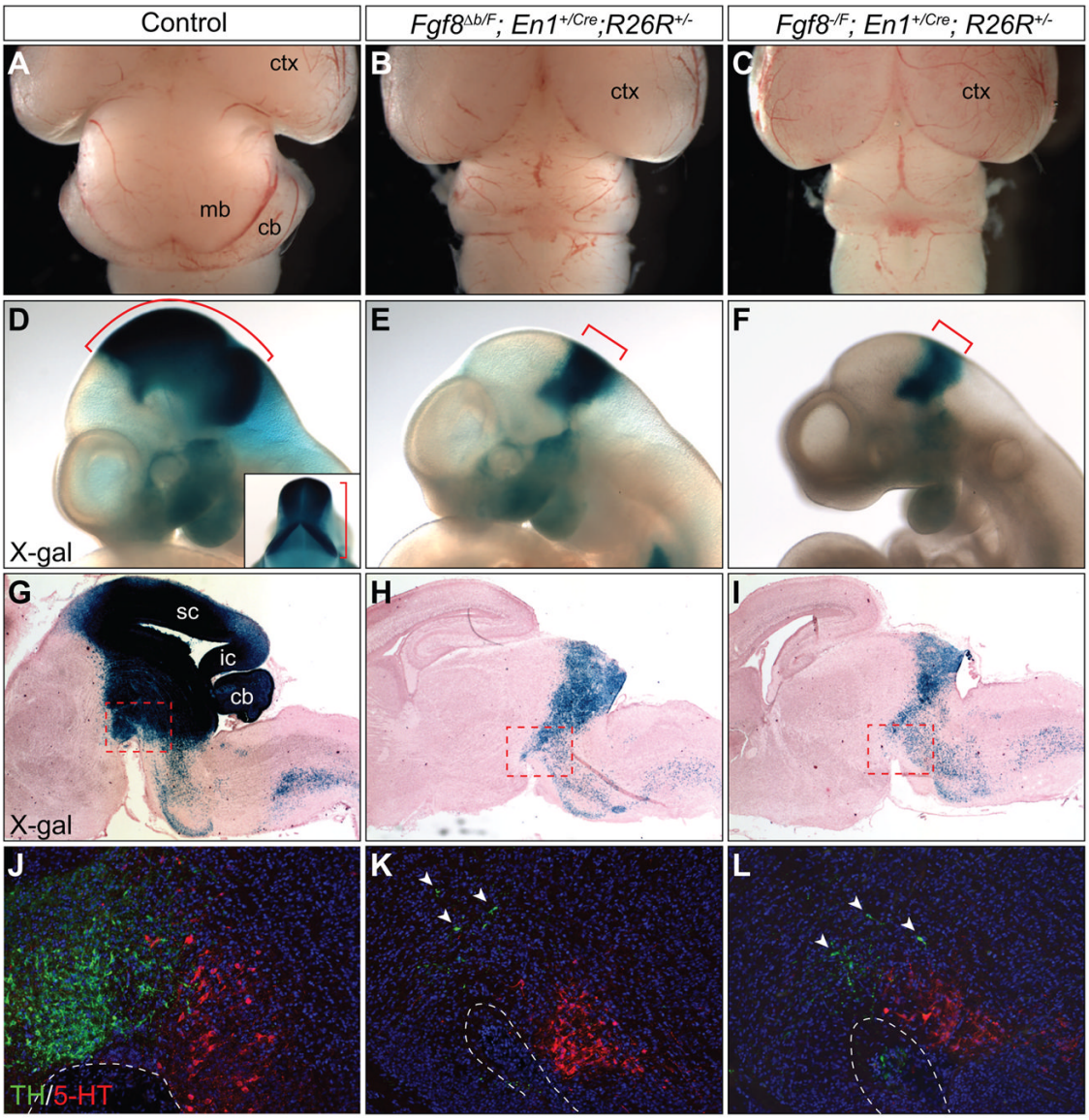

Figure 1. Specific deletion of *Fgf8b* or *Fgf8* in the mes/r1 region results in similar loss of midbrain and hindbrain tissues

(A–C) Dorsal views of E18.5 brains of genotypes as indicated at the top. (D–I) X-gal staining of wholemount embryos at E10.5 (**D–F**) and sagittal sections of E18.5 brains (G–I) of genotypes indicated. Bracket marks the mes/r1 domain. (J–L) Immunofluorescence labeling of dopaminergic (TH) and serotonergic (5-HT) neurons in the ventral midbrain and hindbrain near the MHB junction on sagittal sections of E18.5 brains. The positions J–L are indicated in boxed areas in D–F, respectively. Arrowheads mark the remaining TH-positive neurons in the mutant embryos. Abbreviations: cb, cerebellum; ctx, cerebral cortex; ic, inferior colliculus; mb, midbrain; sc, superior colliculus.

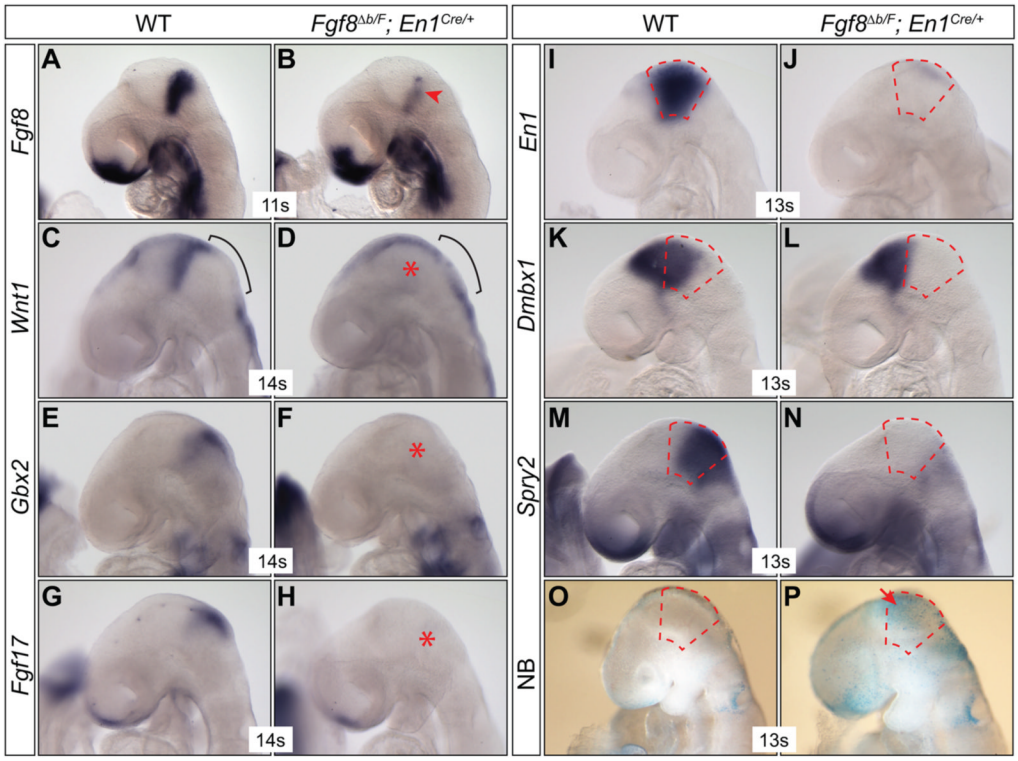

Figure 2. *Fgf8b* is required to maintain expression of mes/r1 genes

(**A**–**N**) In situ hybridization. Probes and genotypes are indicated at the left and top of the panel, respectively. The number of somites is indicated between each pair of control and mutant embryos. A ribroprobe corresponding to a full-length *Fgf8* cDNA is used so that *Fgf8* transcription is analyzed even though exon 3 is deleted by Cre-mediated recombination of $Fgf8^{F}$ allele. Arrowhead marks reduced expression of *Fgf8* at the isthmus in *Fgf8b*-CKO embryos; asterisk indicates the absence of gene expression at the isthmus; bracket demarcates r1 region; dashed line circles the mes-r1 region. (O–P) Nile Blue sulfate staining of dying cells. Arrow indicates increased number of dead cells in the mes.

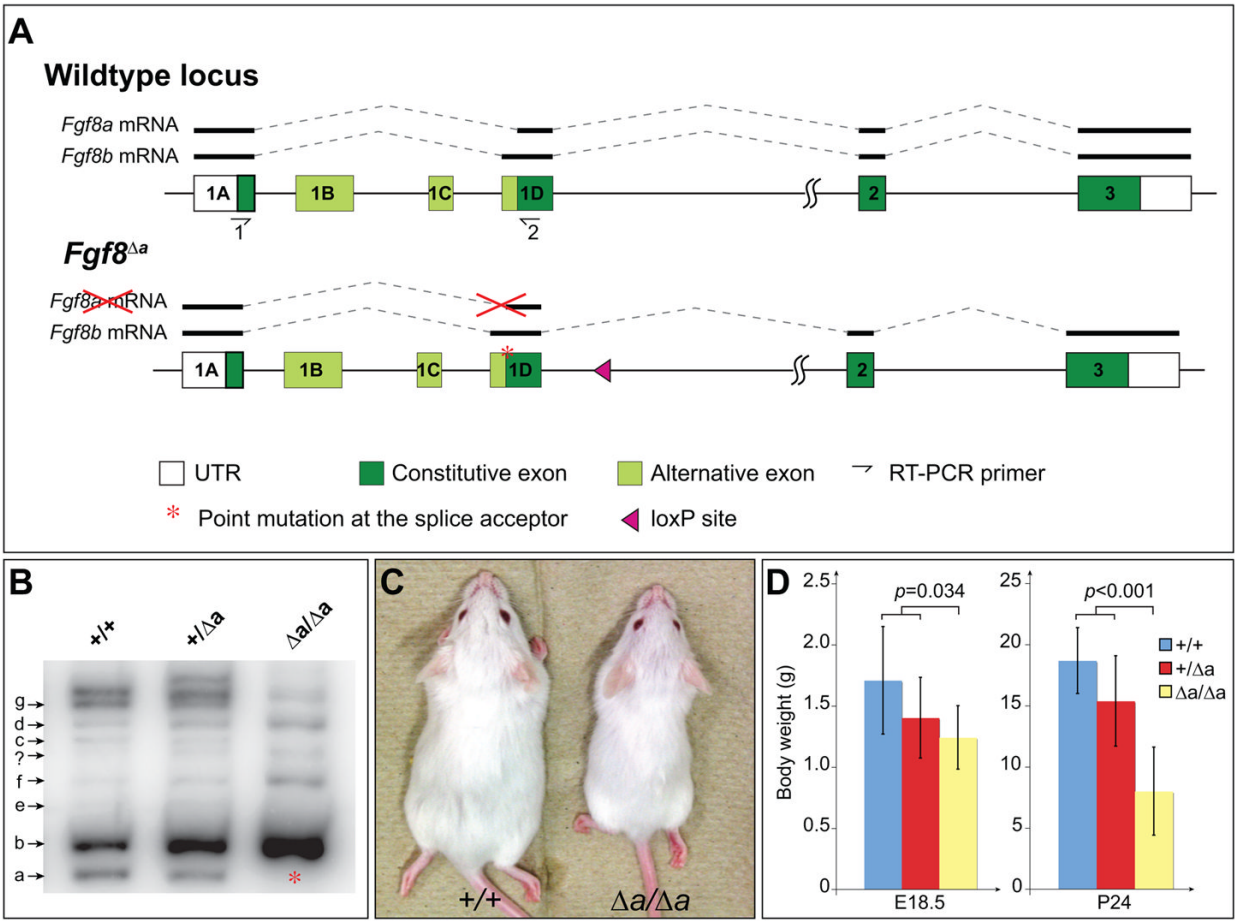

Figure 3. Mutant mice lacking Fgf8a spliceform are retarded in growth

(**A**) Schematic representation of the generation of a mutation deleting *Fgf8a* in mice. (**B**) RT-PCR analysis of spliceforms of *Fgf8* from total RNA of E8.5 embryos. Note that *Fgf8a* transcripts (asterisk) are missing in $Fgf8^{\Delta a/\Delta a}$ embryos, whereas the transcripts of *Fgf8b*, *d*, *f* and *h* appear slightly more abundant compared with those in the controls. Question mark indicates two unknown splice variants of *Fgf8*. (**C**) $Fgf8^{\Delta a/\Delta a}$ mice are smaller in size at 6 weeks old. (**D**) Histogram of the average body weight of $Fgf8^{\Delta a/\Delta a}$ mutants and their littermate controls at E18.5 and P24.

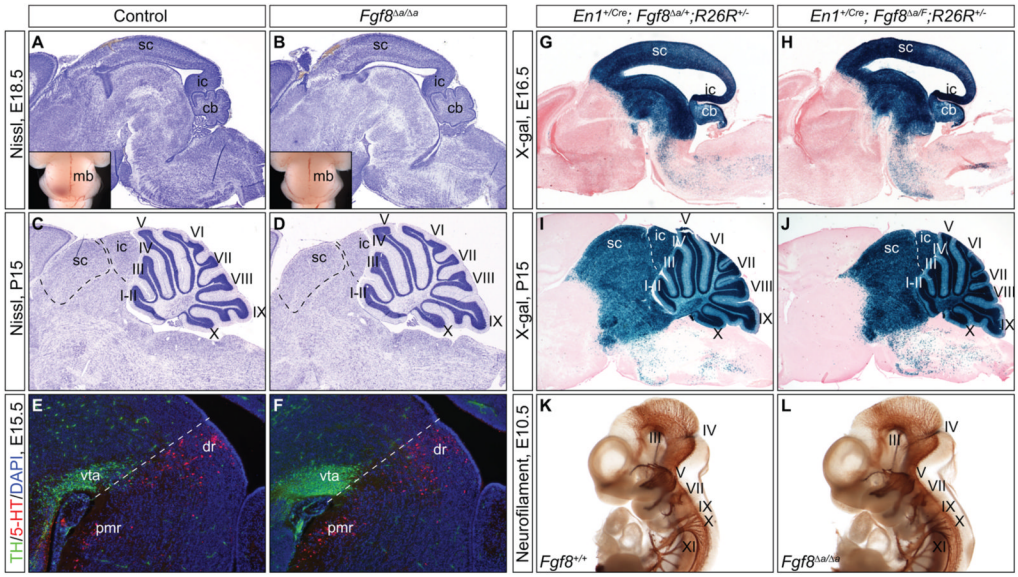

Figure 4. Normal development of the midbrain and hindbrain in mice lacking *Fgf8a*

(**A**–**D**) Nissl staining of sagittal sections of brains at E18.5 (A–B) and P15 (C–D). The genotypes are indicated at the top. Insets show dorsal views of the midbrain and cerebellum. (**E**–**F**) Immunofluorescence of TH and 5-HT positive neurons in the basal plate around the mid-hindbrain junction (dashed line). Arrowhead indicates the junction between the inferior colliculus (ic) and cerebellum (cb). (**G**–**J**) X-gal staining of sagittal sections of brains at E16.5 (G–H) and P15 (I–J). The genotypes are indicated at the top of the panel. (**K**–**L**) Neurofilament immunohistochemistry of cranial nerves (Roman numerals) in wild-type (K) and *Fgf8*$^{\Delta a/\Delta a}$ embryos at E10.5. Abbreviations: dr, dorsal raphe nuclei; mb, midbrain; pmr, paramedial raphe nuclei; sc, superior colliculus; vta, ventral tegmental area.

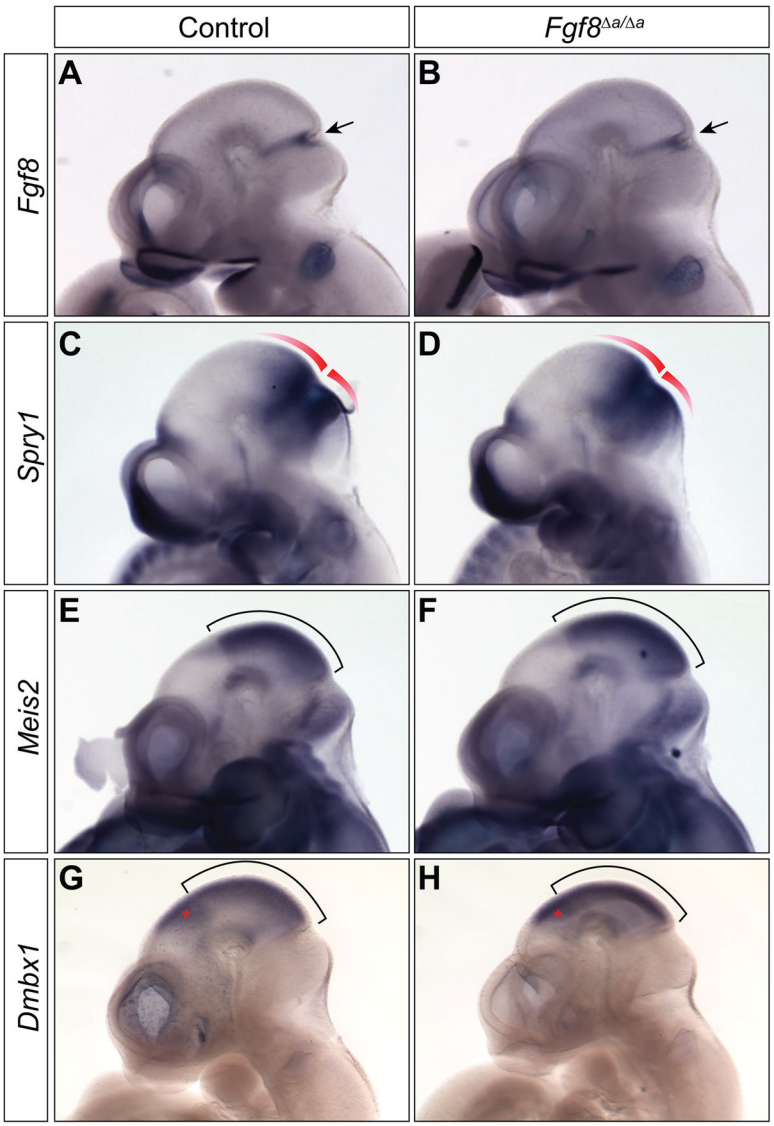

Figure 5. Expression of mes/r1 genes is unaffected in the absence of *Fgf8a*

(**A**–**H**) In situ hybridization of whole-mount embryos at E10.5. The probes and genotypes are indicated to the left and the top, respectively. The range (brackets) and the gradient (boxes) of marker expression in the mes or r1 are indistinguishable between wild-type and *Fgf8*$^{\Delta a/\Delta a}$ embryos. Arrow and asterisk indicate the isthmus and the diencephalon, respectively.

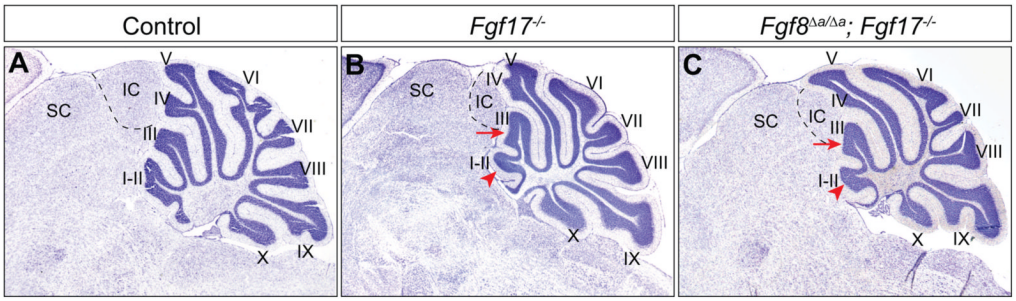

Figure 6. Fgf8a and Fgf17 does not play redundant role in the development of the cerebellum

(**A**–**C**) Nissl staining of sagittal sections of the midbrain and cerebellum of indicated genotypes at about 3 weeks of age. The lobules of the vermis are marked by Roman numerals according to Inouye and Oda (Inouye and Oda, 1980). Red arrowheads and arrows indicate the truncated lobules I–II and III, respectively. Abbreviations: ic, inferior colliculus; sc, superior colliculus.

Table I

Ratio of progeny of different genotypes

			Genotype						
		Mating	**WT**	**Het**	**Homo**	**Total**	**Litters**	**Average litter size**	**Chi square test**
a	CD1	*Fgf8*$^{+/\Delta a}$ × *Fgf8*$^{+/\Delta a}$ (P0-20)	122	201 (4)	86 (14)	427	39	10.9	0.0340
b		*Fgf8*$^{+/\Delta a}$ × *Fgf8*$^{+/\Delta a}$ (E15.5–18.5)	46	108	51	205	16	12.8	0.659
									*0.0389
c	C57BL/6J	*Fgf8*$^{+/\Delta a}$ × *Fgf8*$^{+/\Delta a}$ (P0-20)	40	52*	3 (5)**	71	26	3.9	**3.601×10^{-7}
d		*Fgf8*$^{+/\Delta a}$ × *Fgf8*$^{+/+}$ (P0-20)	57	36 (2)		89	17	5.6	0.029
e		*Fgf8*$^{+/\Delta b}$ × *Fgf8*$^{+/+}$(P0-20)	52	53		105	19	5.5	0.922

Number of dead pups is shown in parenthesis.

Dev Biol. Author manuscript; available in PMC 2011 February 15.